Eur. Phys. J. C (2021) 81:1007
https://doi.org/10.1140/epjc/s10052-021-09778-2

THE EUROPEAN PHYSICAL JOURNAL C

Regular Article - Theoretical Physics

Muon $g-2$ anomaly and μ–τ-philic Higgs doublet with a light CP-even component

Hong-Xin Wang[1], **Lei Wang**[1,a], **Yang Zhang**[2]

[1] Department of Physics, Yantai University, Yantai 264005, People's Republic of China
[2] School of Physics and Microelectronics, Zhengzhou University, Zhengzhou 450001, People's Republic of China

Received: 2 August 2021 / Accepted: 28 October 2021 / Published online: 15 November 2021

Abstract We examine the possibilities of accommodating the muon $g-2$ anomaly released by Fermilab in the 2HDM with a discrete Z_4 symmetry in which an inert Higgs doublet field (H, A, $H^{\pm}$) has the lepton flavor violation μ–τ interactions. We assume the Yukawa matrices to be real and symmetrical and investigate the case of light H (5 GeV $< m_H <$ 115 GeV). After imposing relevant theoretical and experimental constraints, especially for the multi-lepton searches at the LHC, we find that the muon $g-2$ anomaly can be explained within 2σ confidence level in the region of 5 GeV $< m_H <$ 20 GeV, 130 GeV $< m_A$ ($m_{H^{\pm}}$) $<$ 610 GeV, and $0.005 < \rho < 0.014$. Meanwhile, the χ^2_τ fitting the data of lepton flavour universality in the τ decays approaches to the SM prediction.

1 Introduction

The Fermilab collaboration released new result of the E989 for muon anomalous magnetic moment ($g-2$) which now, combined with the measurement of the E821 [1,2], amounts to [3]

$$\Delta a_\mu = a_\mu^{exp} - a_\mu^{SM} = (25.1 \pm 5.9) \times 10^{-10}, \tag{1}$$

which has an approximate 4.2σ discrepancy from the SM prediction.

Two-Higgs-doublet model (2HDM) is a simple extension of SM by including one more electroweak Higgs doublet field. The Δa_μ discrepancy can be easily explained in the lepton-specific 2HDM [4–16] and aligned 2HDM [17–26]. However, in the decay $\tau \to \mu\nu\bar{\nu}$, the tree-level diagram mediated by the charged Higgs gives negative contribution, which will lead to the deviation of the lepton flavor universality (LFU) in τ decays [13–15]. Besides, a scalar with the μ–τ lepton flavor violation (LFV) interactions can accommodate the Δa_μ discrepancy by the one-loop contribution [27–40]. Meanwhile, the extra Higgs doublet with the μ–τ LFV interactions can alleviate the discrepancy of LFU in τ decays [34]. In this paper, we consider relevant theoretical and experimental constraints, including the lepton flavor universality (LFU) in the τ decays and multi-lepton event searches at the LHC, and examine the possibilities of explaining the Δa_μ discrepancy reported by Fermilab in the 2HDM with a discrete Z_4 symmetry in which an inert Higgs doublet field (H, A, $H^{\pm}$) has the lepton flavor violation μ–τ interactions. Ref. [36] applied the model to discuss the E821 result of Δa_μ discrepancy and focused on the case of $m_H >$ 200 GeV. Different from the Ref. [36], in this paper we try to use a light H to explain the muon $g-2$ combining the LFU in the τ decays and multi-lepton event searches at the LHC.

The rest of the paper is organized as follows. In Sect. 2 we introduce the model briefly. In Sect. 3 we discuss the muon $g-2$, the LFU in τ decays, the exclusion limits of multi-lepton event searches at the LHC, and other relevant constraints. In Sect. 4, we show the allowed and excluded parameter space. Finally, we give our conclusion in Sect. 5.

2 The 2HDM with μ–τ-philic Higgs doublet

The SM is extended by adding an inert Higgs doublet ϕ_2 under an abelian discrete Z_4 symmetry, and the Z_4 charge assignment is shown in Table 1 [34].

The scalar potential is expressed as

$$\begin{aligned} V = {} & Y_1(\phi_1^\dagger\phi_1) + Y_2(\phi_2^\dagger\phi_2) + \frac{\lambda_1}{2}(\phi_1^\dagger\phi_1)^2 + \frac{\lambda_2}{2}(\phi_2^\dagger\phi_2)^2 \\ & + \lambda_3(\phi_1^\dagger\phi_1)(\phi_2^\dagger\phi_2) + \lambda_4(\phi_1^\dagger\phi_2)(\phi_2^\dagger\phi_1) \\ & + \left[\frac{\lambda_5}{2}(\phi_1^\dagger\phi_2)^2 + \text{h.c.}\right]. \end{aligned} \tag{2}$$

[a] e-mail: leiwang@ytu.edu.cn (corresponding author)

Table 1 The Z_4 charge assignment of μ–τ-philic 2HDM

	ϕ_1	ϕ_2	Q_L^i	U_R^i	D_R^i	L_L^e	L_L^μ	L_L^τ	e_R	μ_R	τ_R
Z_4	1	-1	1	1	1	1	i	$-i$	1	i	$-i$

Although λ_5 is the only potentially complex parameter, it can be rendered real with a phase redefinition of one of the two Higgs fields. Therefore, λ_5 could be real without loss of generality. The two complex scalar doublets ϕ_1 and ϕ_2 take the form

$$\phi_1 = \begin{pmatrix} G^+ \\ \frac{1}{\sqrt{2}}(v + h + iG^0) \end{pmatrix}, \quad \phi_2 = \begin{pmatrix} H^+ \\ \frac{1}{\sqrt{2}}(H + iA) \end{pmatrix}.$$

The vacuum expectation value (VEV) of the ϕ_1 field is v=246 GeV, while the ϕ_2 field has zero VEV. The Y_1 is calculated using the minimization condition of the scalar potential.

$$Y_1 = -\frac{1}{2}\lambda_1 v^2. \tag{3}$$

The G^0 and G^+ indicate Nambu–Goldstone bosons eaten by the gauge bosons. The A and H^+ represent the mass eigenstates of the CP-odd Higgs boson and charged Higgs boson, whose masses are written as

$$m_{H^\pm}^2 = Y_2 + \frac{\lambda_3}{2}v^2, \quad m_A^2 = m_{H^\pm}^2 + \frac{1}{2}(\lambda_4 - \lambda_5)v^2. \tag{4}$$

Therefore, their masses are

$$m_h^2 = \lambda_1 v^2 \equiv (125 \text{ GeV})^2, \quad m_H^2 = m_A^2 + \lambda_5 v^2. \tag{5}$$

We obtain the masses of fermions via the Yukawa interactions with ϕ_1,

$$-\mathcal{L} = y_u \overline{Q}_L \tilde{\phi}_1 U_R + y_d \overline{Q}_L \phi_1 D_R + y_\ell \overline{L}_L \phi_1 E_R + \text{h.c.} \tag{6}$$

Here $Q_L^T = (u_{Li}, d_{Li})$, $L_L^T = (\nu_{Li}, \ell_{Li})$, and $\widetilde{\phi}_1 = i\tau_2\phi_1^*$, where i is generation index. E_R, U_R, and D_R represent the three generation charged lepton, right-handed fields of the up-type quark and down-type quark, respectively. Under the Z_4 symmetry, the lepton Yukawa matrix y_ℓ to be diagonal. As a result, the lepton fields (L_L, E_R) are mass eigenstates.

Under the Z_4 symmetry, the ϕ_2 is allowed to have μ–τ interactions [34],

$$-\mathcal{L}_{LFV} = \sqrt{2}\,\rho_{\mu\tau}\,\overline{L_L^\mu}\,\phi_2\,\tau_R + \sqrt{2}\,\rho_{\tau\mu}\,\overline{L_L^\tau}\,\phi_2\,\mu_R + \text{h.c.} \tag{7}$$

The interactions of Eq. (7) lead to the μ–τ LFV couplings of H, A, and $H^\pm$.

If the new Yukawa couplings $\rho_{\mu\tau}$ and $\rho_{\tau\mu}$ are complex, the model will give additional contributions to the electric dipole moment (EDM) of muon via the same diagram for muon $g-2$. The current experimental bound on muon EDM is [41]

$$\frac{|\,d_\mu\,|}{e} < 1.9 \times 10^{-19} \text{ cm}, \tag{8}$$

which can impose an upper limit on the imaginary part of $\rho_{\mu\tau}\rho_{\tau\mu}$. For simplicity, we take the CP-conserving Yukawa matrix, namely that $\rho_{\mu\tau}$ and $\rho_{\tau\mu}$ are real.

The SM-like Higgs h has the same tree-level couplings to fermions and gauge boson as the SM, and has no μ–τ LFV coupling. The H, A, and $H^\pm$ have the μ–τ-philic Yukawa couplings and no other Yukawa couplings. There are no cubic interactions with ZZ, WW for the neutral Higgses A and H.

3 Muon $g-2$, LFU in τ decays, LHC data, and relevant constraints

In our numerical calculations, the input parameters are λ_2, λ_3, m_h, m_H, m_A and $m_{H^\pm}$. The values of λ_1, λ_4 and λ_5 can be determined according to Eqs. (4, 5), and m_h is fixed at 125 GeV. The key parameters are scanned over in the following ranges:

$$0 < \rho_{\mu\tau} = \rho_{\tau\mu} \equiv \rho < 1.0,\ 5 \text{ GeV} < m_H < 115 \text{ GeV},$$
$$130 \text{ GeV} < m_A < 900 \text{ GeV},\ 90 \text{ GeV} < m_{H^\pm} < 900 \text{ GeV}. \tag{9}$$

We choose $\rho < 1.0$ to maintain the perturbativity of the new Yukawa couplings. For $m_H < m_A$, the contribution of H to muon $g-2$ can overcome that of A, and leads to a positive contribution to the muon $g-2$. When the mass of H (A) is closed to that of h, the signal data of the 125 GeV Higgs will constrain the couplings of H (A). Therefore, we take $m_H < 115$ GeV and $m_A > 130$ GeV. When m_H is much larger than m_τ, the corresponding contributions to muon $g-2$ can be approximately given by a simple expression. As a result, $m_H > 5$ GeV is taken. Considering the searches for the charged Higgs at the LEP [42], we require $m_{H^\pm} > 90$ GeV.

The λ_2, which controls the quartic couplings of additional Higgses, does not affect the observables studied in this paper. We choose $\lambda_3 = \lambda_4 + \lambda_5$ which leads the hHH coupling to vanish. The tree-level couplings of the SM-like Higgs h to the SM particles are exactly same to the SM, and there is no exotic decay mode. Since the extra Higgses do not couple to quarks, we may safely neglect the bounds of meson observable. HiggsBounds [43] is used to implement the exclusion constraints from the searches for the neutral and charged

Higgs at the LEP at 95% confidence level. In addition, we consider other observables and constraints:

(1) Theoretical constraints and the oblique parameters. We use the 2HDMC [44] to implement the theoretical constraints from the unitarity, vacuum stability and perturbativity of coupling-constant, as well as the oblique parameters (S, T, U). The recent fit results of the oblique parameters [45] are

$$S = 0.02 \pm 0.10, \quad T = 0.07 \pm 0.12, \\ U = 0.00 \pm 0.09, \tag{10}$$

with the correlation coefficients of

$$\rho_{ST} = 0.92, \quad \rho_{SU} = -0.66, \quad \rho_{TU} = -0.86. \tag{11}$$

They favor parameter spaces with small mass splitting between $H^\pm$ and H or A.

(2) Muon $g-2$ anomaly. In the model, the new contribution to Δa_μ comes from the one-loop diagrams containing the μ–τ LFV coupling of H and A [28],

$$\Delta a_\mu = \frac{m_\mu m_\tau \rho^2}{8\pi^2}\left[\frac{(\log\frac{m_H^2}{m_\tau^2}-\frac{3}{2})}{m_H^2} - \frac{\log(\frac{m_A^2}{m_\tau^2}-\frac{3}{2})}{m_A^2}\right]. \tag{12}$$

The Eq. (12) shows that the new contributions are positive for $m_A > m_H$. This is reason why we take $m_A > m_H$ in our calculations.

(3) Lepton universality in the τ lepton decays. The strictest constraints are from the measurements on ratios of pure leptonic processes, and two ratios from semi-hadronic processes, $\tau \to \pi/K\nu$ and $\pi/K \to \mu\nu$,

$$\left(\frac{g_\tau}{g_\mu}\right)^2 \equiv \bar{\Gamma}(\tau \to e\nu\bar{\nu})/\bar{\Gamma}(\mu \to e\nu\bar{\nu}), \\ \left(\frac{g_\tau}{g_e}\right)^2 \equiv \bar{\Gamma}(\tau \to \mu\nu\bar{\nu})/\bar{\Gamma}(\mu \to e\nu\bar{\nu}), \\ \left(\frac{g_\mu}{g_e}\right)^2 \equiv \bar{\Gamma}(\tau \to \mu\nu\bar{\nu})/\bar{\Gamma}(\tau \to e\nu\bar{\nu}), \tag{13}$$

where $\bar{\Gamma}$ denotes the partial width normalized to corresponding SM value. In this model, we have

$$\bar{\Gamma}(\tau \to \mu\nu\bar{\nu}) = (1+\delta^\tau_{\text{loop}})^2\,(1+\delta^\mu_{\text{loop}})^2 + \delta_{\text{tree}}, \\ \bar{\Gamma}(\tau \to e\nu\bar{\nu}) = (1+\delta^\tau_{\text{loop}})^2, \\ \bar{\Gamma}(\mu \to e\nu\bar{\nu}) = (1+\delta^\mu_{\text{loop}})^2. \tag{14}$$

Here δ_{tree} is from the tree-level diagram mediated by the charged Higgs,

$$\delta_{\text{tree}} = 4\frac{m_W^4\rho^4}{g^4 m_{H^\pm}^4}, \tag{15}$$

which can give a positive correction to $\tau \to \mu\nu\bar{\nu}$. δ^μ_{loop} and $\delta^\tau_{\text{loop}}$ are the corrections to vertices $W\bar{\nu_\mu}\mu$ and $W\bar{\nu_\tau}\tau$ from the one-loop diagrams containing A, H, and $H^\pm$, respectively. As we assume $\rho_{\mu\tau} = \rho_{\tau\mu}$ in the lepton Yukawa matrix, we have $\delta^\tau_{\text{loop}} = \delta^\mu_{\text{loop}}$. Following the results of [13,15,34],

$$\delta^\tau_{\text{loop}} = \delta^\mu_{\text{loop}} = \frac{1}{16\pi^2}\rho^2\left[1 + \frac{1}{4}\left(H(x_A) + H(x_H)\right)\right], \tag{16}$$

where $H(x_\phi) \equiv \ln(x_\phi)(1+x_\phi)/(1-x_\phi)$ with $x_\phi = m_\phi^2/m_{H^\pm}^2$.
In our model,

$$\left(\frac{g_\tau}{g_\mu}\right) = \left(\frac{g_\tau}{g_\mu}\right)_K = \left(\frac{g_\tau}{g_\mu}\right)_\pi. \tag{17}$$

The results obtained by the HFAG collaboration are [46]

$$\left(\frac{g_\tau}{g_\mu}\right) = 1.0011 \pm 0.0015, \left(\frac{g_\tau}{g_e}\right) = 1.0029 \pm 0.0015, \\ \left(\frac{g_\mu}{g_e}\right) = 1.0018 \pm 0.0014, \left(\frac{g_\tau}{g_\mu}\right)_\pi = 0.9963 \pm 0.0027, \\ \left(\frac{g_\tau}{g_\mu}\right)_K = 0.9858 \pm 0.0071, \tag{18}$$

with correlation matrix of

$$\begin{pmatrix} 1 & 0.53 & -0.49 & 0.24 & 0.12 \\ 0.53 & 1 & 0.48 & 0.26 & 0.10 \\ -0.49 & 0.48 & 1 & 0.02 & -0.02 \\ 0.24 & 0.26 & 0.02 & 1 & 0.05 \\ 0.12 & 0.10 & -0.02 & 0.05 & 1 \end{pmatrix}. \tag{19}$$

We perform a χ^2_τ fit for the five observables. The eigenvalues of covariance matrix constructed from the data of Eq. (18) and Eq. (19) are absent, so we remove the corresponding degree in the calculation. In following discussions, we require $\chi^2_\tau < \chi^2_\tau|_{\text{SM}} = 12.3$, i.e. giving better explanation than SM.

(4) Lepton universality in the Z boson decays. The experimental values of the ratios of the Z leptonic decay branch-

ing fractions are [47]:

$$\frac{\Gamma_{Z\to\tau^+\tau^-}}{\Gamma_{Z\to e^+e^-}} = 1.0019 \pm 0.0032, \tag{20}$$
$$\frac{\Gamma_{Z\to\mu^+\mu^-}}{\Gamma_{Z\to e^+e^-}} = 1.0009 \pm 0.0028. \tag{21}$$

The correlation coefficient is 0.63. In our model, the new contributions to the decay widths of $Z \to \mu^+\mu^-$ and $Z \to \tau^+\tau^-$ are from the one-loop diagrams containing the extra Higgs bosons. The ratio of Eq. (20) is given as [13,15,34]

$$\frac{\Gamma_{Z\to\tau^+\tau^-}}{\Gamma_{Z\to e^+e^-}} \approx 1.0 + \frac{2g_L^e \mathrm{Re}(\delta g_L^{\mathrm{loop}}) + 2g_R^e \mathrm{Re}(\delta g_R^{\mathrm{loop}})}{{g_L^e}^2 + {g_R^e}^2}, \tag{22}$$

where $g_R^e = 0.23$ and $g_L^e = -0.27$. The one-loop corrections $\delta g_L^{\mathrm{loop}}$ and $\delta g_R^{\mathrm{loop}}$ are from

$$\begin{aligned}
\delta g_L^{\mathrm{loop}} =& \frac{1}{16\pi^2}\rho^2 \Big\{ -\frac{1}{2}B_Z(r_A) - \frac{1}{2}B_Z(r_H) - 2C_Z(r_A, r_H) \\
&+ s_W^2 \Big[B_Z(r_A) + B_Z(r_H) + \tilde{C}_Z(r_A) + \tilde{C}_Z(r_H)\Big]\Big\}, \\
\delta g_R^{\mathrm{loop}} =& \frac{1}{16\pi^2}\rho^2 \Big\{2C_Z(r_A, r_H) - 2C_Z(r_{H^\pm}, r_{H^\pm}) + \tilde{C}_Z(r_{H^\pm}) \\
&- \frac{1}{2}\tilde{C}_Z(r_A) - \frac{1}{2}\tilde{C}_Z(r_H) \\
&+ s_W^2 [B_Z(r_A) + B_Z(r_H) + 2B_Z(r_{H^\pm}) \\
&+ \tilde{C}_Z(r_A) + \tilde{C}_Z(r_H) + 4C_Z(r_{H^\pm}, r_{H^\pm})]\Big\},
\end{aligned} \tag{23}$$

where $r_\phi = m_\phi^2/m_Z^2$, $\phi = A, H, H^\pm$, and

$$B_Z(r) = -\frac{\Delta_\epsilon}{2} - \frac{1}{4} + \frac{1}{2}\log(r), \tag{24}$$
$$\begin{aligned} C_Z(r_1, r_2) =& \frac{\Delta_\epsilon}{4} - \frac{1}{2}\int_0^1 dx \int_0^x dy \log[r_2(1-x) \\ &+ (r_1 - 1)y + xy], \end{aligned} \tag{25}$$
$$\begin{aligned} \tilde{C}_Z(r) =& \frac{\Delta_\epsilon}{2} + \frac{1}{2} - r\big[1 + \log(r)\big] \\ &+ r^2\big[\log(r)\log(1 + r^{-1}) \\ &- \mathrm{Li}_2(-r^{-1})\big] \\ &- \frac{i\pi}{2}\Big[1 - 2r + 2r^2\log(1 + r^{-1})\Big]. \end{aligned} \tag{26}$$

Besides, $\Gamma_{Z\to\mu^+\mu^-}$ equals to $\Gamma_{Z\to\tau^+\tau^-}$ for $\rho_{\mu\tau} = \rho_{\tau\mu}$.
(5) The multi-lepton searches at the LHC. The H, A, and $H^\pm$ are mainly produced at the LHC via the electroweak processes:

$$pp \to W^{\pm *} \to H^\pm A, \tag{27}$$
$$pp \to W^{\pm *} \to H^\pm H, \tag{28}$$
$$pp \to Z^* \to HA, \tag{29}$$
$$pp \to Z^*/\gamma^* \to H^+H^-. \tag{30}$$
$$pp \to Z \to \tau^\pm\mu^\mp H. \tag{31}$$

For compressed spectrum, the main decay modes of H, A, and $H^\pm$ are

$$H \to \tau^\pm\mu^\mp, \quad A \to \tau^\pm\mu^\mp, \quad H^\pm \to \tau^\pm\nu_\mu, \mu^\pm\nu_\tau. \tag{32}$$

For m_A ($m_{H^\pm}$) $> m_H + m_Z$, the following exotic decay modes will open,

$$A \to HZ, \quad H^\pm \to HW^\pm. \tag{33}$$

We use `MG5_aMC-2.4.3` [48] to simulate above processes at 13 TeV LHC, with `PYTHIA6` [49] for parton shower and hadronization, `Delphes-3.2.0` [50] for fast detector simulation, and `Fastjet` [52] for jet reconstruction. Then we impose the constraints from all the ATLAS and CMS analysis at the 13 TeV LHC in the latest `CheckMATE 2.0.28` [51]. The analysis we implemented in our previous works [36,53] are also included. Besides, we implement the recently published analyses of searching for events with final states of three or more leptons using 137 fb^{-1} LHC data [54]. It improves significantly the limits on new physical particles that decay to leptons. The signal regions of `4lI`, `4lJ` and `4lK`, which require 4 leptons with one or two hadronical τ leptons in the final states, are most sensitive to our samples, because the main decay modes of H, A, and $H^\pm$ are lepton dominated.

4 Results and discussions

Firstly, we impose the constraints of "pre-muon $g-2$" (including the theory and the oblique parameters constraints, the exclusion limits from the searches for Higgs at LEP), and display the surviving samples with $\chi^2_\tau < 12.3$ fitting the data of LFU in τ decays in Fig. 1. For a very small ρ, the new contributions to τ decays disappear. Therefore, the value of χ^2_τ approaches to the SM value, 12.3. The discrepancy of LFU in τ decays can be alleviated by enhancing $\Gamma(\tau \to \mu\nu\bar{\nu})$. From Eq. (14), we can find that $\tau \to \mu\nu\nu$ receives the corrections from the one-loop diagram and tree-level diagram mediated by the charged Higgs. According to Eq. (16), the former tends

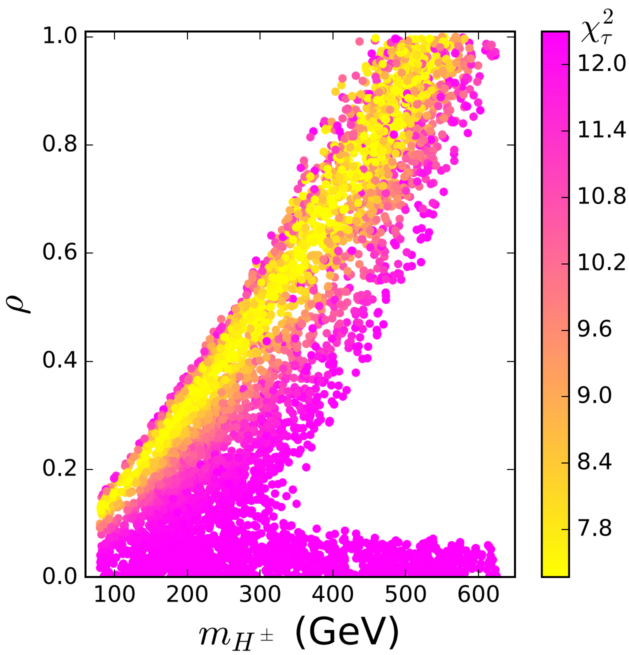

Fig. 1 The surviving samples satisfying the constraints of "pre-muon $g-2$" and $\chi^2_\tau < 12.3$ projected on the plane of ρ versus $m_{H^\pm}$

to give the negative corrections and enhance the value of χ^2_τ. According to Eq. (15), the latter gives the positive corrections and reduce the value of χ^2_τ. In order to obtain $\chi^2_\tau < 12.3$ for a large $m_{H^\pm}$, a large ρ is required to make the contributions of tree-level diagram to overcome those of one-loop diagram since the contributions of tree-level diagram are suppressed by $m_{H^\pm}$. For $\chi^2_\tau < 9.7$, ρ is always required to increase with $m_{H^\pm}$ and be larger than 0.11.

After further imposing the constraints of muon $g-2$ anomaly, we project the surviving samples on the planes of ρ versus m_H and ρ versus Δm ($\Delta m = m_A - m_H$) in Fig. 2. From the Eq. (12), we can find that Δa_μ receives a positive correction from the diagrams containing H and a negative correction from ones involving A. As a result, Δa_μ is sizable enhanced by a large mass splitting between m_A and m_H (Δm), and favors ρ to decrease with an increase of Δm, as shown in the right panel of Fig. 2. In addition, the Eq. (12) shows that the contributions of the diagrams containing H and A to Δa_μ are respectively suppressed by m_H^2 and m_A^2. Therefore, Δa_μ favors ρ to increase with m_H, as shown in the left panel of Fig. 2. The Δa_μ discrepancy can be explained in the parameter space of $0.005 < \rho < 0.12$ and 5 GeV $< m_H <$ 115 GeV.

In Fig. 3, we show the surviving samples after imposing the constraints of "pre-muon $g-2$", muon $g-2$, $\chi^2_\tau < 12.3$, and Z decays. Since the muon $g-2$ anomaly favors $0.005 < \rho < 0.12$, most of the parameter space satisfying $\chi^2_\tau < 12.3$ are excluded. From Fig. 3, we find that a small χ^2_τ favors a large m_H and a small $m_{H^\pm}$. Since the Δa_μ discrepancy favors a large ρ for a large m_H, and such large ρ can enhance the width of $\tau \to \mu\nu\nu$ and reduce the value of χ^2_τ.

After imposing the constraints of the direct searches at the LHC, the surviving samples of Fig. 3 are projected on Fig. 4. We find that the direct searches at the LHC impose a stringent upper bound on m_H, $m_H <$ 20 GeV, and allow 130 GeV $< m_A$ ($m_{H^\pm}$) $<$ 610 GeV. It is caused by the multi-lepton searches described in Sect. 3, especially the CMS searches for the direct production of charginos and neutralinos in signatures with two/three or more leptons [54,55]. The most sensitive signal regions require four leptons including up to two hadronically decaying tau leptons, as in our model the HA pair production leads to $\tau\tau\mu\mu$ final state. However, for a light H, the $\tau\mu$ from H decays become too soft to be distinguished at detector, while the $\tau\mu$ from H in $A/H^\pm$ decays are collinear because of the large mass splitting between H and $A/H^\pm$. In addition, in the low m_H region, the $A/H^\pm \to HZ/W^\pm$ decays can dominate over the $A \to \tau\mu$ and $H^\pm \to \tau\nu_\mu, \mu\nu_\tau$. Thus, in the region of $m_H <$ 20 GeV, the acceptance of above signal region for final state containing collinear $\tau\mu + Z/W$ boson quickly decreases. For 5 GeV $< m_H <$ 20 GeV, the Δa_μ discrepancy favors $0.005 < \rho < 0.014$. As a result, the new contributions to the τ decays are very small, and the χ^2_τ approaches to the value of SM, 12.3.

In our calculation, we always assume $\rho_{\mu\tau} = \rho_{\tau\mu}$. If the relation is not satisfied, the ρ^2 in the Eq. (12) for Δa_μ is replaced with $\rho_{\mu\tau}\rho_{\tau\mu}$. For the calculation of LFU in τ decays, the ρ^4 of the Eq. (15) for δ_{tree} is replaced with $\rho^2_{\mu\tau}\rho^2_{\tau\mu}$, and the one-loop correction $\delta^\tau_{\text{loop}}$ does not equal to the δ^μ_{loop}. For the calculation of the Z decays, the ρ^2 of the Eq. (23) for δg_L^{loop} and δg_R^{loop} are respectively replaced with $\rho^2_{\tau\mu}$ and $\rho^2_{\mu\tau}$. If one of $|\rho_{\mu\tau}|$ and $|\rho_{\tau\mu}|$ is very small, the other is required to be large enough to explain the muon $g-2$ and LFU in τ decays, which is more easily constrained by the perturbativity and Z decays than the case of $\rho_{\mu\tau} = \rho_{\tau\mu}$.

In order to fit the observed data of neutrino masses and mixings, the Z_4 flavor symmetry in the model must be broken [34,56]. One may introduce a SM singlet scalar S with Z_4 charge i and three right-handed neutrinos (N_{eR}, $N_{\mu R}$, $N_{\tau R}$) with $(1,\ i,\ -i)$. The interaction terms relevant to neutrino sector are then given by

$$
\begin{aligned}
-\mathcal{L}_N = {} & \frac{1}{2}\left(\overline{N^c_{eR}}\ \overline{N^c_{\mu R}}\ \overline{N^c_{\tau R}}\right)\begin{pmatrix} M_1 & y_{12}S^* & y_{13}S \\ y_{12}S^* & & M_{23} \\ y_{13}S & M_{23} & \end{pmatrix}\begin{pmatrix} N_{eR} \\ N_{\mu R} \\ N_{\tau R}\end{pmatrix} \\
& + \left(\overline{L_e}\ \overline{L_\mu}\ \overline{L_\tau}\right)\begin{pmatrix} y_{e1}\phi_1 & & \\ & y_{\mu 2}\phi_1 & y_{\mu 3}\phi_2 \\ & y_{\tau 2}\phi_2 & y_{\tau 3}\phi_1 \end{pmatrix}\begin{pmatrix} N_{eR} \\ N_{\mu R} \\ N_{\tau R}\end{pmatrix} \\
& + \text{h.c.}
\end{aligned} \tag{34}
$$

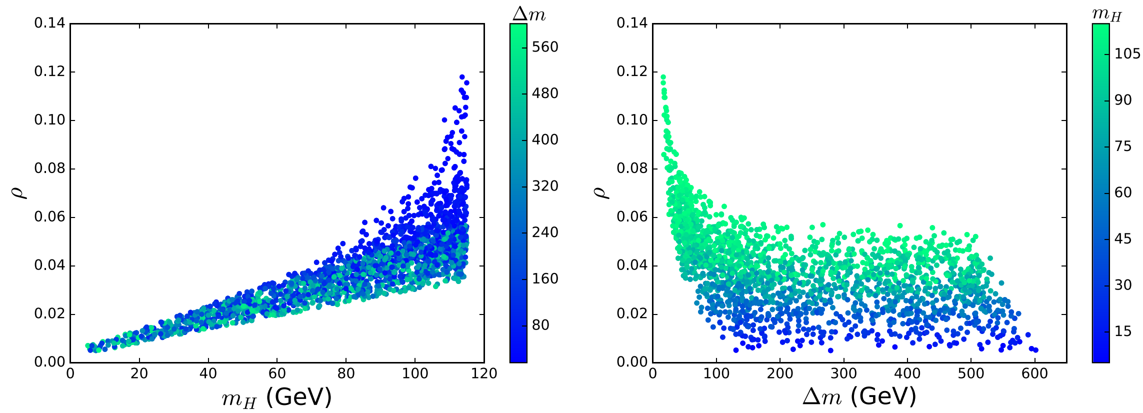

Fig. 2 The surviving samples satisfying the constraints of "pre-muon $g-2$" and muon $g-2$ anomaly projected on the planes of ρ versus m_H and ρ versus Δm

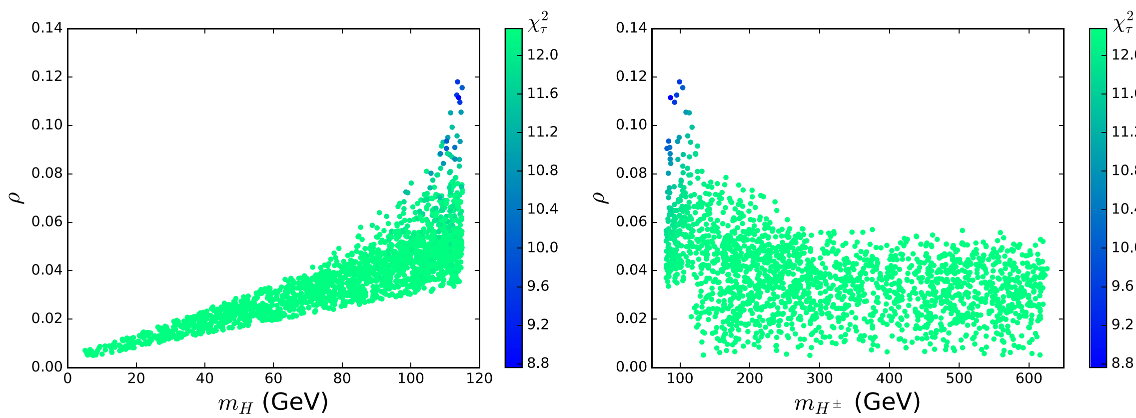

Fig. 3 The surviving samples satisfying the constraints of "pre-muon $g-2$", muon $g-2$ anomaly, $\chi^2_\tau < 12.3$, and Z decays

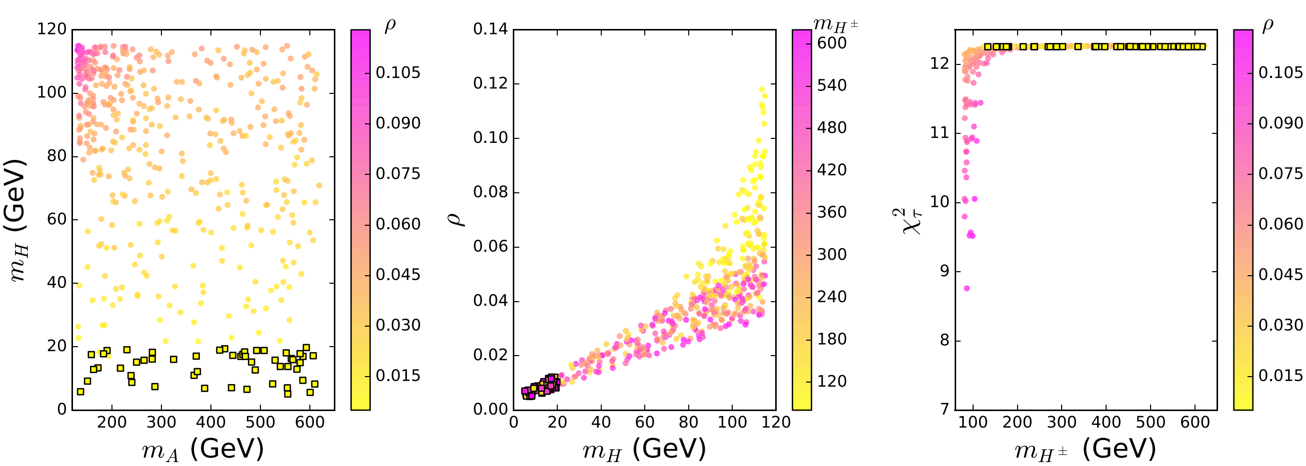

Fig. 4 The surviving samples on the planes of m_H versus m_A, ρ versus m_H, and χ^2_τ versus $m_{H^\pm}$. All the samples satisfy the constraints of "pre-muon $g-2$", muon $g-2$ anomaly, $\chi^2_\tau < 12.3$, and Z decays. The bullets and squares are excluded and allowed by the direct searches at the LHC

We assume the singlet S to have a VEV ε, which breaks the Z_4 symmetry. Thus, the total neutrino mass matrix has the structure

$$M_\nu \propto \begin{pmatrix} \mathcal{O}(\varepsilon^0) & \mathcal{O}(\varepsilon) & \mathcal{O}(\varepsilon) \\ \mathcal{O}(\varepsilon) & \mathcal{O}(\varepsilon^2) & \mathcal{O}(\varepsilon^0) \\ \mathcal{O}(\varepsilon) & \mathcal{O}(\varepsilon^0) & \mathcal{O}(\varepsilon^2) \end{pmatrix}. \quad (35)$$

At the leading order of $\mathcal{O}(\varepsilon^0)$, the neutrino mass matrix has non-zero values only in (1, 1), (2, 3), and (3, 2) elements. We can diagonalize this mass matrix by using a unitary matrix (PMNS matrix). Because of the vanishing (2, 2) and (3, 3) elements at the order of $\mathcal{O}(\varepsilon^0)$, the model can naturally predict a large θ_{23} mixing angle. Therefore, such extension of model can relax the constraints of neutrino data sizably.

5 Conclusion

In the 2HDM with an abelian discrete Z_4 symmetry, one Higgs doublet has the same interactions with fermions as the SM, and another inert Higgs doublet only has the μ–τ LFV interactions. After imposing various relevant theoretical and experimental constraints, especially for the multi-lepton search at the LHC, we found that the model can explain the Δa_μ discrepancy within 2σ confidence level in the region of $5\,\text{GeV} < m_H < 20\,\text{GeV}$, $130\,\text{GeV} < m_A\ (m_{H^\pm}) < 610\,\text{GeV}$, and $0.005 < \rho < 0.014$. Meanwhile, the χ^2_τ fitting the data of LFU in the τ decays approaches to the SM prediction.

Acknowledgements This work was by the National Natural Science Foundation of China under grant 11975013 and 12105248, and by the Project of Shandong Province Higher Educational Science and Technology Program under Grants No. 2019KJJ007.

Data Availability Statement This manuscript has associated data in a data repository. [Authors' comment: All data used in this publication are available from the corresponding author on reasonable request].

Funded by SCOAP[3].

References

1. Muon g-2 Collaboration, Phys. Rev. Lett. **86**, 2227 (2001)
2. Muon g-2 Collaboration, Phys. Rev. D **73**, 072003 (2006)
3. B. Abi et al. [Fermilab Collaboration], Phys. Rev. Lett. **126**, 141801 (2021)
4. A. Dedes, H.E. Haber, JHEP **0105**, 006 (2001)
5. D. Chang, W.-F. Chang, C.-H. Chou, W.-Y. Keung, Phys. Rev. D **63**, 091301 (2001)
6. K.M. Cheung, C.H. Chou, O.C.W. Kong, Phys. Rev. D **64**, 111301 (2001)
7. J. Cao, P. Wan, L. Wu, J.M. Yang, Phys. Rev. D **80**, 071701 (2009)
8. L. Wang, X.F. Han, JHEP **05**, 039 (2015)
9. E.J. Chun, Z. Kang, M. Takeuchi, Y.-L. Tsai, JHEP **1511**, 099 (2015)
10. A. Cherchiglia, P. Kneschke, D. Stockinger, H. Stockinger-Kim, JHEP **1701**, 007 (2017)
11. X. Liu, L. Bian, X.-Q. Li, J. Shu, Nucl. Phys. B **909**, 507–524 (2016)
12. X.-F. Han, T. Li, L. Wang, Y. Zhang, Phys. Rev. D **99**, 095034 (2019)
13. T. Abe, R. Sato, K. Yagyu, JHEP **1507**, 064 (2015)
14. A. Crivellin, J. Heeck, P. Stoffer, Phys. Rev. Lett. **116**, 081801 (2016)
15. E.J. Chun, J. Kim, JHEP **1607**, 110 (2016)
16. L. Wang, J.M. Yang, M. Zhang, Y. Zhang, Phys. Lett. B **788**, 519–529 (2019)
17. T. Han, S.K. Kang, J. Sayre, JHEP **1602**, 097 (2016)
18. V. Ilisie, JHEP **1504**, 077 (2015)
19. O. Eberhardt, A. Martínez, A. Pich, arXiv:2012.09200
20. S.-P. Li, X.-Q. Li, Y. Li, Y.-D. Yang, X. Zhang, JHEP **2101**, 034 (2021)
21. S.-P. Li, X.-Q. Li, Y.-D. Yang, Phys. Rev. D **99**, 035010 (2019)
22. N. Ghosh, J. Lahiri, arXiv:2103.10632
23. S. Jana, P.K. Vishnu, S. Saad, Phys. Rev. D **101**, 115037 (2020)
24. N. Chen, B. Wang, C. Yao, arXiv:2102.05619
25. F.J. Botella, F. Cornet-Gomez, M. Nebot, Phys. Rev. D **102**, 035023 (2020)
26. E.J. Chun, T. Mondal, Phys. Lett. B **802**, 135190 (2020)
27. K. Adikle Assamagan, A. Deandrea, P.-A. Delsart, Phys. Rev. D **67**, 035001 (2003)
28. S. Davidson, G.J. Grenier, Phys. Rev. D **81**, 095016 (2010)
29. Y. Omura, E. Senaha, K. Tobe, JHEP **1505**, 028 (2015)
30. R. Benbrik, C.-H. Chen, T. Nomura, Phys. Rev. D **93**, 095004 (2016)
31. Y. Omura, E. Senaha, K. Tobe, Phys. Rev. D **94**, 055019 (2016)
32. M. Lindner, M. Platscher, F.S. Queiroz, Phys. Rep. **731**, 1–82 (2018)
33. L. Wang, S. Yang, X.-F. Han, Nucl. Phys. B **919**, 123–141 (2017)
34. Y. Abe, T. Toma, K. Tsumura, JHEP **1906**, 142 (2019)
35. S. Iguro, Y. Omura, M. Takeuchi, JHEP **1911**, 130 (2019)
36. L. Wang, Y. Zhang, Phys. Rev. D **100**, 095005 (2019)
37. S. Iguro, Y. Omura, M. Takeuchi, JHEP **09**, 144 (2020)
38. A. Crivellin, D. Müller, C. Wiegand, JHEP **06**, 119 (2019)
39. A. Das, Ti. Nomura, H. Okada, Phys. Rev. D **96**, 075001 (2017)
40. P.S.B. Dev, R.N. Mohapatra, Y. Zhang, Phys. Rev. Lett **120**, 221804 (2018)
41. G.W. Bennett et al. [Muon (g-2) Collaboration], Phys. Rev. D **80**, 052008 (2009)
42. G. Abbiendi et al. [ALEPH and DELPHI and L3 and OPAL and LEP Collaborations], Eur. Phys. J. C **73**, 2463 (2013)
43. P. Bechtle, O. Brein, S. Heinemeyer, G. Weiglein, K.E. Williams, Comput. Phys. Commun. **181**, 138–167 (2010)
44. D. Eriksson, J. Rathsman, O. Stål, Comput. Phys. Commun. **181**, 189 (2010)
45. M. Tanabashi et al. [Particle Data Group], Phys. Rev. D **98**, 030001 (2018)
46. Y. Amhis et al. [Heavy Flavor Averaging Group (HFAG) Collaboration], arXiv:1412.7515

47. S. Schael et al. [ALEPH and DELPHI and L3 and OPAL and SLD and LEP Electroweak Working Group and SLD Electroweak Group and SLD Heavy Flavour Group Collaborations], Phys. Rep. **427**, 257 (2006)
48. J. Alwall et al., JHEP **1407**, 079 (2014)
49. P. Torrielli, S. Frixione, JHEP **1004**, 110 (2010)
50. J. de Favereau et al. [DELPHES 3 Collaboration], JHEP **1402**, 057 (2014)
51. D. Dercks, N. Desai, J.S. Kim, K. Rolbiecki, J. Tattersall, T. Weber, Comput. Phys. Commun. **221**, 383 (2017)
52. M. Cacciari, G.P. Salam, G. Soyez, Eur. Phys. J. C **72**, 1896 (2012)
53. G. Pozzo, Y. Zhang, Phys. Lett. B **789**, 582–591 (2019)
54. A.M. Sirunyan et al. [CMS Collaboration], CMS-PAS-SUS-19-012
55. A.M. Sirunyan et al. [CMS Collaboration], JHEP **03**, 166 (2018)
56. K. Asai, K. Hamaguchi, N. Nagata, Eur. Phys. J. C **77**, 763 (2017)